Colloid Polym Sci (2006) 284: 489–496
DOI 10.1007/s00396-005-1407-1

ORIGINAL CONTRIBUTION

Mohamed Kasseh
Erlend Keh

The binding of benzyldimethyldodecylammonium bromide to acrylamide-co-sodium-2-acrylamido-2-methylpropanesulfonate copolymers: thermodynamical and conformational aspects

Received: 30 May 2005
Accepted: 18 July 2005
Published online: 11 November 2005

M. Kasseh · E. Keh (✉)
LAMMI, UMR-5072CNRS,
Université Montpellier II,
Place Eugène Bataillon,
34095 Montpellier Cedex 5, France
e-mail: e.keh@univ-montp2.fr
Tel.: +33-4-673243
Fax: +33-4-67143304

Present address:
M. Kasseh
Medin Tech,
6644 Abrams,
St. Laurent H4S 1Y1, Canada

Abstract The binding isotherms of benzyldimethyldodecylammonium bromide (BDDAB) to copolymers of acrylamide and sodium-2-acrylamido-2-methylpropanesulfonate (AMPS), 5 or 20% in mole ratios (AMPS5 and AMPS20, respectively), are determined by membrane ultrafiltration and analysed with the Satake–Yang formalism in terms of binding constants and cooperativities. Complexation is further investigated by steady-state fluorescence of solubilized pyrene, dynamic light scattering (DLS) and laser Doppler electrophoresis (LDE). Hydrophobic aggregates bound to AMPS20 appear similar to BDDAB free micelles, whereas those borne by AMPS5 increase in size more distinctly under the non-stoichiometric complexation mechanism. Multimolecular association and dissociation equilibria are displayed by DLS in the AMPS5 biphasic domain. Above the critical aggregation concentration, electrophoretic mobilities of the complexes initially remain unchanged by compensation of antagonistic electrostatic contributions. Upon progressive binding of micelles the charge-to-friction ratio of the polyons is reduced by condensation of the counter-ions.

Keywords Anionic–nonionic copolymers · Benzyldimethyldodecylammonium bromide · Binding isotherms · Light scattering · Pyrene fluorescence · Electrophoretic mobilities

Introduction

Polyelectrolytes and charged surfactants encompass distinct physical features and relevant applications. When opposite in sign their association is well documented [1, 2], which can display new rheological behaviors, synergistic surface effects [3, 4], or nano-scale structures [5–7]; developments in these fields were recently reviewed [8]. Benefiting from early theoretical works, the interactions of strong polyelectrolytes with oppositely charged surfactants have focused substantial interest sustained by experimental determinations of binding isotherms issued from the development of surfactant-selective membrane electrodes [9, 10]. Progress in the understanding of electrostatic and hydrophobic contributions to the binding mechanisms has fostered investigations of surfactant-polyelectrolyte complexes and nanostructures, correlatively stimulating the design of polymer gels as potential actuators [11, 12]. Okuzaki, Osada and Gong have systematically investigated the interactions of *N*-alkyl-pyridinium chlorides to solubilized or cross-linked poly [(2-(acrylamido)-2-methylpropanesulfonic acid] [13–16]. They characterized the binding of the surfactant by a two-step mechanism, along which an initial one-to-one (stoichiometric) electrostatic ion exchange was followed by a cooperative hydrophobic association of the hitherto singly bound surfactant cations, producing an insoluble stoichiometric complex. Alternatively, the copolymer of 2-acrylamido-2-methylpropanesulfonate (AMPS) and isopropylacrylamide (10 mol%), in the presence of lauryl pyridinium chloride, precipitates but redissolves upon reaching the critical micelle concentration (CMC) of the surfactant. Such mechanism, due to the onset of a non-stoichiometric association, was unveiled by monitoring the yield of precipitate in conjunction with the binding iso-

therm [17]; alternatively it was anticipated from gel shrinking and reswelling profiles [17, 18] or a variation of the viscosity [19].

As a preliminary to further interaction of our system with solid particles, we investigate here the binding processes of BDDAB to AMPS5 and AMPS20, which illustrate similar diverging phase separation evolutions at much lower linear charge density. Complexation isotherms are obtained by tangential flow ultrafiltration and UV spectroscopy. Further insights into the bound clusters formation and development in relation to the copolymer specificity are obtained by fluorescence spectroscopy of solubilized pyrene. The association and conformational variations of the macro-ions upon surfactant addition are accounted for by dynamic light scattering (DLS) and laser Doppler electrophoresis (LDE).

Experimental section

Chemicals

AMPS5 and AMPS20 (SNF, Saint-Etienne, France) were used as received. The average molecular weight (M_w) of AMPS5 is specified as 10^7 g mol^{-1}. From light-scattering measurements, the Zimm plot of AMPS20 in 0.1 M NaCl yielded M_w=4.9 10^6 g mol^{-1} and a gyration radius of 280 nm. The dilute/semi-dilute transitions of the higher- and lower-sulfonated homologs were located at 0.04 mg g^{-1} by rheology and 0.24 mg g^{-1} by conductimetry, respectively. BDDAB (Fluka) was successively recrystallized from ethylacetate (Aldrich) and from water. Its CMC is 5.6×10^{-3} M. Using dynamic back-scattering of light (HPPS instrument, Malvern) a Z average micelle hydrodynamic diameter of 3.6 nm was obtained from a 13-mM BDDAB aqueous solution. Pyrene (Aldrich) was recrystallized three times from ethanol (Merck). Ultra-high-quality water was used throughout (Elga, France).

Sample preparation

Solutions were prepared at a constant copolymer concentration of 1.0 mg g^{-1} [(AMPS20)=1.94 mM)] and 0.18 mg g^{-1} [(AMPS5)=0.115 mM] for AMPS20 and AMPS5, respectively. Copolymer-surfactant mixtures were adjusted by weight from a stock solution of copolymer, water and a BDDAB stock solution sparingly added under fast stirring. Magnetic stirring in closed vials was maintained during at least 24 h to reach equilibrium. In the biphasic regions, supernatants were separated from the precipitates by centrifugation at 10,000 rpm (tabletop instrument). Samples probed by LDE and DLS were similarly spun for 30 min, the latter being those previously used for the binding determinations.

Binding isotherms

Separation between free and polymer-bound surfactants was achieved by ultrafiltration using a polyethersulfone hollow fibre membrane (400 kDa M_w cut-off) inserted into a MicroKros module of ca. 0.5 ml dead volume (both from Spectrum, the Netherlands). Tangential flow extraction was produced by hand-operated syringes. From a 20-ml feed volume, 0.5 ml of filtrate was extracted and analysed by UV spectroscopy (Cary 3E, Varian) to quantify the free BDDAB concentration using the benzyl moiety vibronic absorption maximum at 268.6 nm (ε=287 l mol^{-1} cm^{-1}). The spread between determinations reached 5%, and the average of 3 was retained. Preliminary assays showed pure BDDAB solutions filtrates to be in agreement with their feed, whereas the leakage of macromolecules remained very marginal in the absence or in the presence of surfactant; the latter imperviousness was monitored by the BDDAB 268/231 nm absorption ratio, which is sensitive to the prominent absorbance of the copolymers at lower wavelengths. As observed by varying the filtrate to membrane contact time, the slow Donnan kinetics does not significantly shift the concentration of the surfactant extract from its copolymer equilibrium value in the feed.

Fluorescence probing

Pyrene concentration was set at 2×10^{-7} M using a solution of pyrene in ethanol either directly injected (0.1% v/v ethanol) into the copolymer-surfactant sample then oven-heated to 50°C or solvent-evaporated from the vial before sample introduction. Mixtures were stirred at least 24 h. Steady-state fluorescence emission (Jobin–Yvon–Spex, Fluoromax 2 instrument) excited at 330 nm with 5- and 0.4-nm excitation and emission slit widths was recorded using a 4-s integration time. Neither residual ethanol nor undissolved solid pyrene contributed significantly to the measurements.

Dynamic light scattering

These determinations were carried out at the scattering angle of 90° with a Zetamaster 3000 HS instrument (Malvern), which employs a 10-mW, 633-nm He–Ne laser, an avalanche photodiode detector and a 256-channel digital correlator. We mostly used a variant of the Contin analysis of the auto-correlation functions as included in the software. From each of the distribution modes of the relaxation times distribution, a mean relaxation time was extracted as the first moment of the normalized relaxation spectrum. The corresponding translation diffusion coefficient D introduced in the following Stokes–Einstein equation yields an apparent hydrodynamic radius R_h along $R_h = kT/6\pi\eta D$, where k is Boltzmann's constant, T is the absolute temper-

ature and η is the solvent viscosity taken as that of water in the following.

Laser Doppler electrophoresis

These measurements were obtained with the same above-mentioned instrument working in the heterodyne detection mode, the counter electro-osmosis flow of the closed cell being subtracted through the fast field reversion instrumental procedure.

Results and discussion

Binding isotherms

Binding of surfactant ions to a polyon of an opposite sign is successively a reversible stoichiometric counter-ion exchange followed by a cooperative process [13]. Inasmuch as the native counter-ion is displaced by a one-to-one exchange, the overall surfactant-binding constant [19], K, to the polyelectrolyte can be modelled as $K=K_0u$, introducing K_0 as the surfactant-binding constant to isolated sites (counter-ion exchange) of a linear polyon and u, the 'cooperative parameter', as the hydrophobic interaction between adjacently bonded neighbours.

Writing here C, C_f and C_{AMPS} for the concentrations of surfactant, free surfactant and sulfonate groups, respectively, the degree of binding, $\beta = (C - C_f)/C_{AMPS}$, was evaluated by Satake and Yang [20] as

$$\beta = 1/2 + (s-1)/2\left[(s-1)^2 + 4s/u\right]^{1/2} \quad (1)$$

with $s=K_0uC_f$

The particular value β=0.5 leads to

$$K = K_0u = (1/C_f)_{0.5} \quad (2)$$

and

$$(\partial\beta/\partial \ln C_f)_{0.5} = u^{1/2}/4 \quad (3)$$

enabling the determination of u and K_0.

Binding isotherms of both copolymers are displayed in Fig. 1, short of the inaccessible early statistical (non-cooperative) regime. The steep sigmoid-shaped binding profile to AMPS20 is significant of a cooperativity that leads bound hydrophobes to form micelle-like clusters wrapped and linked by the macromolecule acting as a source of counter-ions [21–24]. Correlatively, the latter spatial configuration shrinks, as supported by the drastic fall of AMPS20 specific viscosity (Fig. 2). The cooperative mechanism saturates at β=1 consistently with a one-to-one stoichiometric

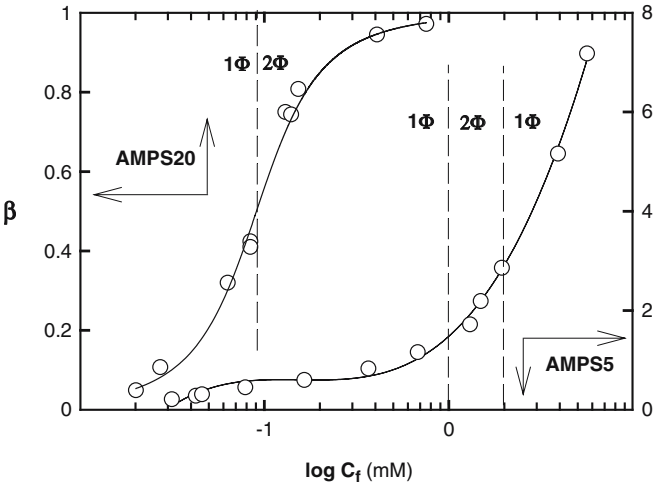

Fig. 1 Binding isotherms of BDDAB to AM-AMPS copolymers as a function of the free surfactant concentration. *Curves* are guides to the eye

exchange which, bearing various interpretations, is found to be less extensive with high linear charge density polyelectrolytes. Precipitation of these complexes starts at a surfactant to AMPS molar ratio r=0.5, whereas destabilization of AMPS5 complexes occurs as r reaches 12, associating a comparatively higher β value. At lower C_f of the latter isotherm, the completion of a weakly cooperative process is obscured by the outset of a non-stoichiometric cooperativity which drastically enhances the binding over β=1 through and past the biphasic region. Total solubility of the solid is recovered when r=20, at variance with the AMPS20 precipitate, which dissolves in the presence of about 1 M NaCl but resists dissolution by excess surfactant. In this

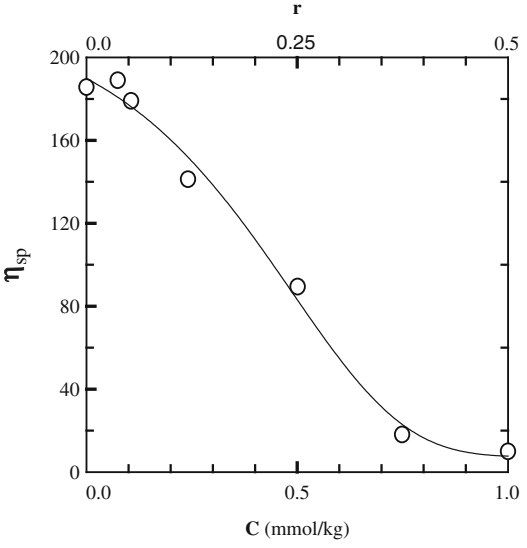

Fig. 2 Variation of the specific viscosity of AMPS20 with BDDAB concentration; Physica UDS 200 instrument, Couette geometry cell, 7.6 s^{-1} steady shear at 25°C

connection, the long acrylamide loops protruding from AMPS5-borne micelles seem likely to impede the stability and order of their micelle-like solid structures [25] in regard of those possibly generated by AMPS20. The wet solid interspaces between AMPS20-clustered micelles could behave as a concentrated micro-electrolytic domain [26, 27] with a high salting-out effectiveness and a lowered water activity restricting surfactant access. By overcoming these factors at a high concentration, NaCl penetration would result in a statistical displacement of some bound sulfonates by chloride ions, whereas the limited chemical potential increase in the free surfactant might not suffice to activate the non-stoichiometric association regime.

As summarized in Table 1, the corresponding modelled K, K_o and u interaction parameters are determined from a fit of [1].

Binding cooperativity increases with polyon linear charge density, surfactant hydrophobicity and added salt concentration, whereas the latter effect depresses K_o as opposed to hydrophobicity [13, 28, 29]. The binding to AMPS5 is close to being non-cooperative (i.e. u=1), whereas AMPS20 cooperativity is considerably reduced, set against the poly-AMPS (3×10^{-3} M)/dodecyl pyridinium chloride system (u=630), notwithstanding the nearly three times inferior CMC of our surfactant [15]. The binding constant of the latter system (K_0=44 l mol^{-1}) is much weaker than that of BDDAB to the more dilute AMPS5. Low linear charge densities induce low statistics of vicinal sulfonates; the occurrence of two successive AMPS groups in AMPS20 is near 2% whatever the synthesis conversion ratio [30]. The deviation between K_o values (Table 1) is assigned to the stronger statistical adsorption competition of native sodium counter-ions, which are comparatively much in excess with AMPS20.

Steady-state fluorescence probing of the complexes

Pyrene's solubility and fluorescence emission quantum yield are markedly enhanced in apolar media as compared to water. Moreover, the I_1/I_3 intensity ratio of its first to third vibronic emission peaks near 373 and 384 nm, respectively, is sensitive to the fluorophor environment [31].

Noticeably, in Fig. 3, the spread of the sigmoid intensity ratio variation is tenfold more extended for AMPS5. The conspicuous onset of the decaying I_1/I_3 profile is ascribed to the critical aggregation concentration (CAC), i.e. to the formation of the early cooperative hydrophobic clusters. The related BDDAB/AMPS molar ratios, r, can be assessed at r=0.09 and r=0.005 for AMPS5 and AMPS20, respectively. These figures set the CAC at 0.01 mM for both copolymers; compared to AMPS5, the higher concentration of AMPS20 native counter-ions opposes and oversizes contributions of an increased charge density to a lowering of the CAC [29, 32].

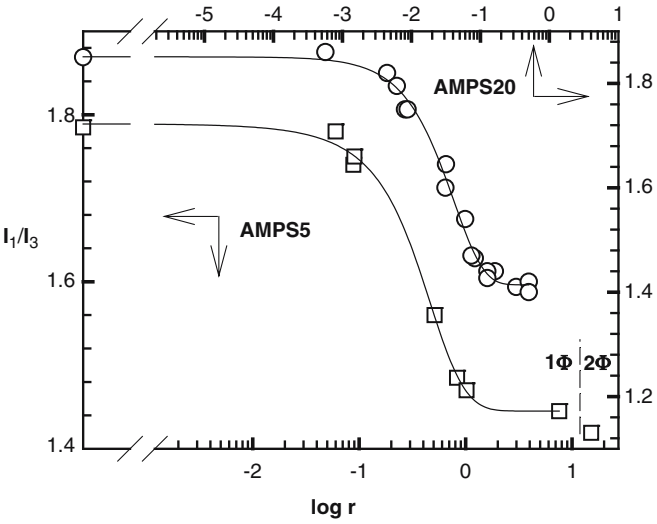

Fig. 3 The I_1/I_3 fluorescence emission intensity ratio of solubilized pyrene as a function of the BDDAB/AMPS molar ratio in the copolymers solutions, T=25°C. *Curves* are to guide the eye

The intensity ratio $(I_1/I_3)_{20}$ of AMPS20 reaches the lower constant value of 1.41 for $r\geq0.2$, indicating total solubility and constant environment of the probe. This value, which is close to the 1.42 figure obtained in 10^{-2} M pure surfactant solution, is also adjoining the 1.40 and 1.42 ratios reported for dodecyl and hexadecyl trimethyl ammonium chloride, respectively. Such comparatively high ratios among ionic micelles are ascribed to an electrostatic attraction between pyrene and the positive cationic surfactant heads, leading the probe to a water-permeated exposure [33]. In the corresponding environment, $(I_1/I_3)_5$=1.44 at r=7.5, but the excess over the AMPS20 figure recedes to 1.42 in the non-stoichiometric cooperative regime at r=15.

The above considerations support a more hydrated environment of the surfactant polar heads in AMPS5 stoichiometric complexes compared to those of AMPS20. Indeed, bulky curls of hydrophilic AMPS5 acrylamide sequences between sulfonate counter-ions are likely to enlarge the polar head surface area at the micelle periphery. The partition of over-stoichiometric surfactants with their bromide counter-ions into these micelles should relax excluded volume and entropic constraints between the latter sequences, resulting in a better screening of the surfactant charges, which enable the building of larger aggregates

Table 1 Overall binding constants K, binding constants to isolated sites K_0 and cooperativity parameters u of BDDAB to AM-AMPS copolymers[a]

Copolymer	$10^{-3}K$ (l mol^{-1})	$10^{-3}K_0$ (l mol^{-1})	u
AMPS5	10	8.2	1.2
AMPS20	10.5	1.7	5.7

[a]Mean square deviations on K_0 and u are ±14% and near ±11% with AMPS20 and AMPS5, respectively

(see under "Electrophoretic mobilities"). Whereas the environmental perturbation produced by these incorporated bromides bear upon the significance of the $(I_1/I_3)_5$ decay between r=7.5 and r=15, the drastic upturn of the AMPS5 isotherm past r=10 substantiate a large enhancement of the initial cooperativity. This view is compatible with the increase in aggregation numbers with binding cooperativity and polyanion linear charge density observed with polyelectrolytes of higher charge densities [32, 34].

Dynamic laser scattering

Further insight into the non-stoichiometric cooperativity was obtained by investigating AMPS5 supernatants by DLS. The inset of Fig. 4 illustrates a typical bimodal relaxation time distribution obtained by Contin analysis at r=19.9, threshold of complete redissolution of the complexes. Such associated fast and slow mean characteristic modes were previously obtained by Fundin et al. when studying the binding of sodium dodecyl sulfate to acrylamide-(3-(2-methylpropionamide) propyl) trimethylammonium chloride [35]. An extensive DLS analysis confirmed these modes as associated to translation diffusivities of single and associated macro-ion complexes, assuming this connection here leads to 87 and 206 nm as the corresponding apparent Stokes–Einstein radii. These both reduce in size at r=13.2 (Fig. 5), while only a single mode appears at r=15.4. In the absence of surfactant, the gyration radius R_g of a single chain can be approximated geometrically by $R_g^3=M_w/(4/3)\pi N_a C^*$, which returns 255 nm using the AMPS5 M_w and overlap concentration (C^*) figures. In this regard, the prominent contribution of

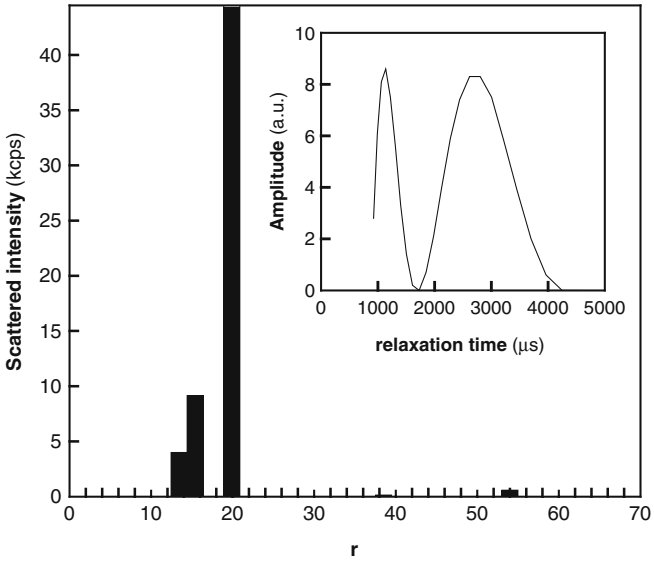

Fig. 4 Variation of the scattered intensity of BDDAB-AMPS5 complexes with the BDDAB/AMPS molar ratio. *Inset*, characteristic time distribution at r=19.9

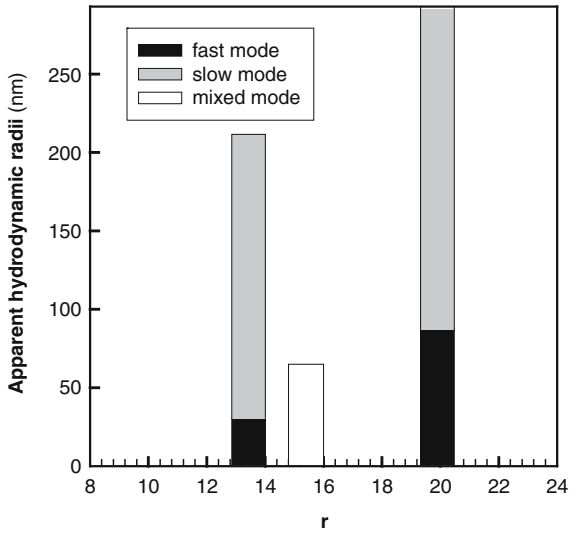

Fig. 5 Apparent DLS radii of complexes observed in the BDDAB-AMPS5 biphasic domain. Relative amplitudes of fast to slow modes are 2.4 and 0.76 at r=13.4 and 19.9, respectively

the 30.5-nm correlation length together with the low scattering intensity observed at r=13.4 (Fig. 5 and legend) are compatible with a contracted single chain. Further surfactant complexation expands the configuration of both single and multichain associates at r=19.9 (Fig. 5), producing a comparatively drastic enhancement of the scattering intensity at a mainly equal solubilized copolymer concentration. Most of the latter has precipitated at r=15.4, which leads us to ascribe the corresponding single mode to large collapsing multichain associates. As r increases, the progressive swelling of the macro-ions lowers their optical contrast to such extent as to render the scattering marginally detectable at r=38 (Fig. 4); the slight intensification produced at r=54 presumably originates from the presence of polymer-free BDDAB micelles since the CMC is exceeded.

Electrophoretic mobilities

These are displayed vs the free surfactant concentration in Fig. 6. The free solution electrophoretic mobility of low-charge-density polyelectrolytes is poorly documented in relation to congruence between theory and experiment. At low concentration in absence of salt, hydrodynamic interactions between charged monomers bring forth a hydrodynamic friction coefficient proportional to the spatial dimension of the coil [36]. Our AMPS5 sample seems more relevant to this view than the surfactant-free AMPS20 solution, the Debye length of which (10 nm) is relatively ten times smaller. The seemingly moderate mobility difference observed here in the absence of surfactant between polyons is mainly ascribable to the more effective counter-ion retarding electro-osmotic flow,

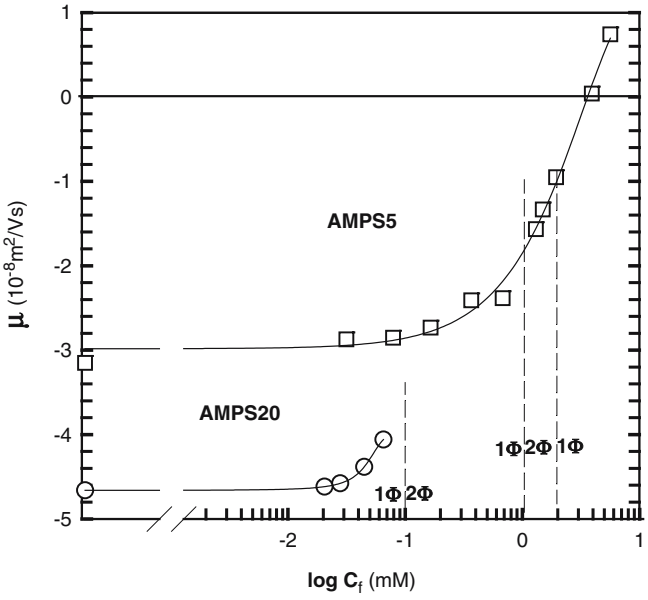

Fig. 6 Electrophoretic mobilities of copolymers vs the log of free surfactant concentration. *Curves* are to guide the eye

which bears upon the motion of AMPS20. Indeed, the latter mobility was found to reach 7.0×10^{-4} cm^2 $V^{-1}s^{-1}$ at 0.075 mM. Using 1.25 nm as the charge interdistance and the sodium counter-ion concentration to evaluate the Debye length, Manning's theoretical mobility value without asymmetric (relaxation) field correction is 5% short of the AMPS20 experimental figure at 1.94 mM but much higher offline at the lower concentration which deviates from the model premises [37]. The specific contribution of its weakly entangled state does not emerge from the former mobility conjunction.

Upon surfactant addition, mobilities remain quasi-invariant until the outset of a declining regime, which leads both copolymers towards precipitation. The turning point of each decay matches the onset of the corresponding I_1/I_3 fluorescence lower plateau, the related characteristic parameters estimates being r=0.12, β=0.1 and I_1/I_3=1.43 for AMPS20 and r=1.5, β=0.6 and I_1/I_3=1.45 for AMPS5. Retraction of polyons configurations is moderate at this stage, considering that AMPS20 viscosity has barely fallen one sixth of the total drop induced by surfactant addition (Fig. 2). As the exchange of the native sodium counter-ions by isolated or sparsely associated BDDAB cations is unlikely to modify substantially the screening of the sulfonates [38], the constant charge-to-friction ratio seems an inconspicuous compensation of the reducing Debye length on both the charge and the configuration of the contracting macro-ions. The following AMPS20 sharp rise of β associated to the corresponding drop of the viscosity and the pyrene-probing observations are consistent with a substantial numerical development of bound micelles, which enhances the screening of the polyon negative charge as more sulfonate counter-ions condense upon the assembled cationic surfactant heads. This major contribution supplementing the increase in free ions would override the reduced friction arising from single or associated contracted coils and thus lower the mobility. Drawing towards the phase-separation boundary, inter-macromolecular association through polyon bridges between micelles is likely to occur, as observed with AMPS5 by DLS. Increasing the inter-aggregate ionic strength would conjecturally enhance the screening of micelles and promote hydrogen bonding between dehydrated acrylamide moieties, inducing a collapse of the clusters. Contrasting with AMPS20, the complete decline and sign reversal of AMPS5 is controlled by further incorporation of free surfactant cations into initial cooperative micelles, the bromides substituting for the sulfonates counter-ions, enabling concurrently the latter to promote new associates. Until interchain linkages develop near C_f=1 mM (r=12), the macro-ion mobility is but weakly reduced. After complete redissolution of the precipitate, single macromolecules expand, bearing progressively less sulfonate counter-ions per bound micelle, which leads to sign reversal. At this stage, one out of five counter-ions is a sulfonate that tethers micelles to polyons; this ratio is yet far from the lower limit foreseen by DLS.

Conclusion

The fourfold excess of acrylamide units between charged groups in AMPS5 over those in AMPS20 gives rise to distinct physico-chemical behaviors of the polyons upon binding of the BDDAB surfactant. Membrane ultrafiltration is shown to be suitable to determine the binding isotherms; the latter are adequately fitted to the Satake–Yang model, which leads to the surfactant-binding constant K_0 and cooperative parameter u. Binding to AMPS20 clearly illustrates the stoichiometric exchange of the native sodium counter-ion by the surfactant cation. Cooperativity is weakly exhibited by the latter and vanishing with its homolog. Deviations between K_0 values together with the identical CACs determined by pyrene fluorescence probing conform to the expected incidence of polyon concentration. Solubilized pyrene experiences the same environment in AMPS20-bound BDDAB micelles than in BDDAB or other cationic micelles in the absence of polyon. AMPS5-bound associates appear to increase in size with the surfactant concentration in the non-stoichiometric regime but starting smaller than the cooperative aggregates of AMPS20 and reaching a similar size. Entangled AMPS20 and dilute AMPS5 chains display parallel variations of their electrophoretic mobility upon the binding of BDDAB. In the absence or presence of sparsely cooperative bonding, Debye charge screening and configuration retraction are both mild and yield balancing

contributions to a mostly flat mobility. The outset of a substantial numerical development of hydrophobic associates and inter-macromolecular bridges leads to a large contraction of the polyons, the reduced friction of which is oversized by the enhanced charge screening issued from the condensation of micelle counter-ions. As monitored by DLS, redissolution of AMPS5 precipitate by excess surfactant induces multichain dissociation and macro-ion expansion that promote a further decline of the mobility towards sign reversal.

References

1. Hayakawa K, Kwak J (1991) Interactions between polymers and cationic surfactants. In: Rubingh D, Holland PM (eds) Cationic surfactants: physical chemistry, surfactant science series, vol 37. Dekker, New York, p 189
2. Lindman B, Thalberg K (1993) Polymer-surfactant interactions—recent developments. In: Goddard ED, Ananthapadmanabhan KP (eds) Interactions of surfactants with polymers and proteins. CRC, Boca Raton, chaps 4–5
3. Maloney C, Huber KJ (1994) Mixtures of polyacrylic acid and nonionic surfactants at the air–water interface. J Colloid Interface Sci 164:463
4. Bergeron V, Langevin D, Asnacios A (1996) Thin-film forces in foam films containing anionic polyelectrolyte and charged surfactants. Langmuir 12:1550
5. Khandurina YV, Dembo AT, Rogacheva VB, Zezin AB, Kabanov VA (1994) Polym Sci USSR 36:189
6. Ober CK, Wegner G (1997) Polyelectrolyte-surfactant complexes in the solid-state: facile building blocks for self-organizing materials. Adv Mater 9:17
7. Zhou S, Burger C, Yeh F, Chu B (1998) Charge density effect of polyelectrolyte chains on the nanostructures of polyelectrolyte-surfactant complexes. Macromolecules 31:8157
8. Tripathy SK, Kumar J, Nalwa HS (eds) (2002) Handbook of polyelectrolytes and their applications, vol 1. American Scientific, Stevenson Ranch
9. Hayakawa K, Kwak JCT (1983) Study of surfactant-polyelectrolyte interactions. 2. Effect of multivalent counterions on the binding of dodecyltrimethyammonium ions by sodium dextran sulfate and sodium poly(styrenesulfonate) in aqueous solution. J Phys Chem 87:506
10. Takisawa N, Hall DG, Wyn-Jones E, Brown P (1988) The construction and characteristics of drug-selective electrodes. Applications for the determination of complexation constants of inclusion complexes with α- and β-cyclodextrins including a kinetic study. J Chem Soc Faraday Trans 1 84:3059
11. Khorkhlov AR, Kramarenko EY, Makhaeva EE, Starodubtzev SG (1992) Collapse of polyelectrolyte networks induced by their interaction with oppositely charged surfactants. Makromol Chem Theory Simul 1:105
12. Okuzaki H, Osada Y (1993) A chemomechanical polymer gel with electrically driven motility. J Intell Mater Syst Struct 4:50
13. Okuzaki H, Osada Y (1994) Effects of hydrophobic interaction on the cooperative binding of a surfactant to a polymer network. Macromolecules 27:502
14. Okuzaki H, Osada Y (1994) Electrodriven polymer gels with biomimetic motility. Polym gels Netw 2:267
15. Okuzaki H, Osada Y (1995) Role and effect of cross-linkage on the polyelectrolyte–surfactant interactions. Macromolecules 28:4554
16. Gong JP, Osada Y (1995) Theoretical analysis of the cross-linking effect on the polyelectrolyte–surfactant interaction. J Phys Chem 99:10971
17. Matsukata M, Hirata M, Gong JP, Osada Y, Sakurai Y, Okano T (1998) Two-step surfactant binding of solvated and cross-linked poly(*N*-isopropylacrylamide-co-(2-acrylamide-2-methyl propane sulfonic acid)). Colloid Polym Sci 276:11
18. Travaš-Sejdić J, Easteal AJ (2000) Equilibrium swelling of poly(AAm-co-AMPS) gels in surfactant solutions. Polymer 41:7451
19. Mylonas Y, Staikos G (2001) Study of the complexation of sodium dodecylsulfate with cationically charged acrylamide and *N*-isopropylacrylamide based copolymers: the role of the polymer chain hydrophobicity and of its charge density. Langmuir 17:3586
20. Satake I, Yang JT (1976) Interaction of sodium decyl sulfate with poly(L-ornithine) and poly(L-lysine) in aqueous solution. Biopolymers 15:2263
21. Chu DY, Thomas JKJ (1986) Effect of cationic surfactants on the conformation transition of poly(methacrylic acid). J Am Chem Soc 108:6260
22. Dubin PL, Rigsbee DR, Mcquigg DWJ (1985) Turbidimetric and dynamic light scattering studies of mixtures of cationic polymers and anionic mixed micelles. J Colloid Interface Sci 105 (2):509
23. Thalberg K, Lindman B (1989) Interaction between hyaluronan and cationic surfactants. J Phys Chem 93:1478
24. Seki M, Morishima Y, Kamachi M (1992) Characterization of the complexes of amphiphilic polyanions and double-chain cationic surfactants. Macromolecules 25:6540
25. Kim B, Ishizawa M, Gong J, Osada Y (1999) Molecular and supramolecular structures of complexes formed by polyelectrolyte-surfactant interactions: effects of charge density and compositions. J Polym. Sci Part A: Polymer Chemistry 37:635
26. Reščič J, Linse P (2001) Gas–liquid phase separation in charged colloidal systems. J Chem Phys 114:10131
27. Thalberg K, Lindman B, Karlström G (1991) Phase behavior of a system of cationic surfactant and anionic polyelectrolyte: the effect of salt. J Phys Chem 95:6004
28. Hayakawa K, Fukutome T, Satake I (1990) Solubilization of water-insoluble dye by a cooperative binding system of surfactant and polyelectrolyte. Langmuir 6:1495
29. Hansson P, Almgren M (1995) Polyelectrolyte-induced micelle formation of ionic surfactants and binary surfactant mixtures studied by time-resolved fluorescence quenching. J Phys Chem 99:16684
30. McCormick CL, Chen GS (1982) Water-soluble copolymers. IV. Random copolymers of acrylamide with sulfonated comonomers. J Polym Sci Polym Chem Ed 20:817
31. Kalyanasundaram K, Thomas JKJ (1977) Environmental effects on vibronic band intensities in pyrene monomer fluorescence and their application in studies of micellar systems. J Am Chem Soc 99:2039

32. Hansson P, Almgren M (1996) Interaction of C_n TAB with sodium (carboxymethyl)cellulose: effect of polyion linear charge density on binding isotherms and surfactant aggregation number. J Phys Chem 100:9038
33. Lianos P, Viriot M-L, Zana R (1984) Study of the solubilization of aromatic hydrocarbons by aqueous micellar solutions. J Phys Chem 88:1098
34. Hansson P, Almgren M (1995) Large C12TAB Micelles formed in complexes with polyvinylsulfate and dextran sulfate. J Phys Chem 99:16694
35. Fundin J, Brown W, Iliopoulos I, Claeson PM (1999) The interaction between sodium dodecylsulfate and the cationic-nonionic random copolymer (3-(2-methylpropionamide)propyl) trimethylammonium chloride-acrylamide of two different charge densities studied using dynamic light scattering and rheometry. Colloid Polym Sci 277:25
36. Long D, Dobrynin AV, Rubinstein M, Adjari A (1998) Electrophoresis of polyampholytes. J Chem Phys 108: 1234
37. Manning GS (1981) Limiting laws and counterion condensation in polyelectrolyte solutions. 7. Electrophoretic mobility and conductance. J Phys Chem 85:1506
38. Miura N, Dubin PL, Moorefield CN, Newkome GR (1999) Complex formation by electrostatic interaction between carboxyl-terminated dendrimers and oppositely charged polyelectrolytes. Langmuir 15:4245